

## Supporting Information

### Magnetic Transition in Exotic Perovskites Stabilized by Chemical and Physical Pressure

Yalin Ma,<sup>a</sup> Maxim S. Molokeev,<sup>b,c,d</sup> Chuanhui Zhu,<sup>a</sup> Shuang Zhao,<sup>a</sup> Yifeng Han,<sup>a</sup> Meixia Wu,<sup>a</sup> Sizhan Liu,<sup>e</sup> Trevor A. Tyson,<sup>e</sup> Mark Croft<sup>f</sup> and Man-Rong Li\*,<sup>a</sup>

<sup>a</sup>. *Key Laboratory of Bioinorganic and Synthetic Chemistry of Ministry of Education, School of Chemistry, Sun Yat-Sen University, Guangzhou 510275, China*

<sup>b</sup>. *Laboratory of Crystal Physics, Kirensky Institute of Physics, Federal Research Center KSC SB RAS, Krasnoyarsk 660036, Russia*

<sup>c</sup>. *Siberian Federal University, Krasnoyarsk 660041, Russia*

<sup>d</sup>. *Department of Physics, Far Eastern State Transport University, Khabarovsk 680021, Russia*

<sup>e</sup>. *Department of Physics, New Jersey Institute of Technology, Newark, New Jersey 07102, United States*

<sup>f</sup>. *Department of Physics & Astronomy, Rutgers, The State University of New Jersey, 136 Frelinghuysen Road, Piscataway, New Jersey 08854, United States*

## **Supplementary Experimental Details**

### **EDS analysis**

Energy Dispersive X-Ray Spectroscopy (EDS) was performed to obtain information on the elemental compositions and atomic percentage.  $\text{Ca}_{2-x}\text{Mn}_x\text{MnTaO}_6$  ( $x = 0.4, 0.6, 0.8$  and  $1.0$ ) are presented as typical examples. Before scanning process, all samples were dried and coated with gold to strengthen the electron conductivity. For every sample, 3 grains were probed; we take the average of three measuring atomic percentage on the basis of EDS peaks. The Ca/Mn/Ta ratios of  $\text{Ca}_{2-x}\text{Mn}_x\text{MnTaO}_6$  are summarized in Table S1.

## Supplementary Figures

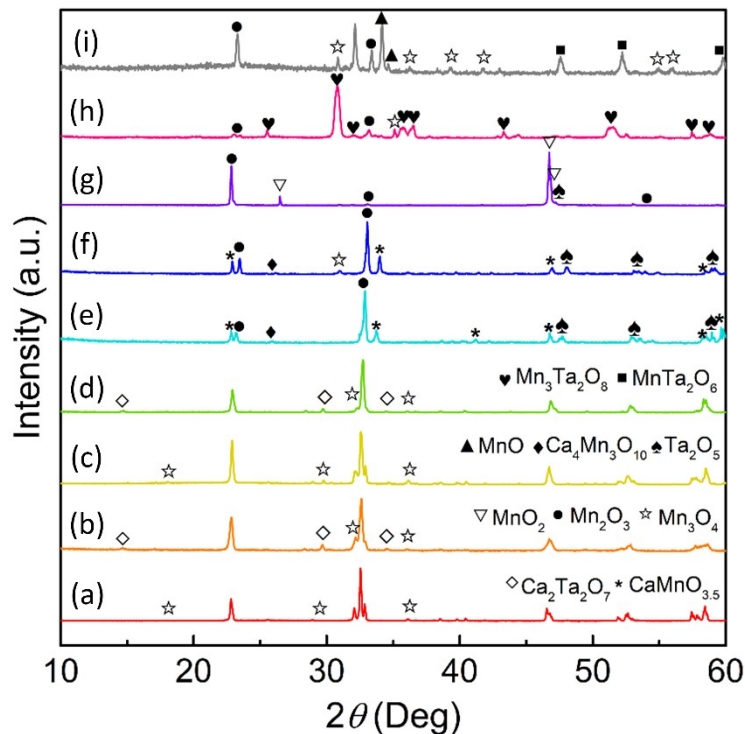


**Fig. S1** X-ray powder diffraction patterns of  $\text{Ca}_{2-x}\text{Mn}_x\text{MnTaO}_6$ : (a)  $x = 0.4$  at 1623 K under AP; (b)  $x = 0.4$  at 1623 K under 5 GPa; (c)  $x = 0.6$  at 1623 K under AP; (d)  $x = 0.6$  at 1623 K under 5 GPa; (e)  $x = 1.5$  at 1623 K under 7 GPa; (f)  $x = 1.6$  at 1623 K under 7 GPa; (g)  $x = 2.0$  at 1573 K under 7 GPa; (h)  $x = 2.0$  at 1623 K under 7 GPa; (i)  $x = 2.0$  at 1523 K under 8 GPa. Signals of the impurity phases are remarked by different symbols.

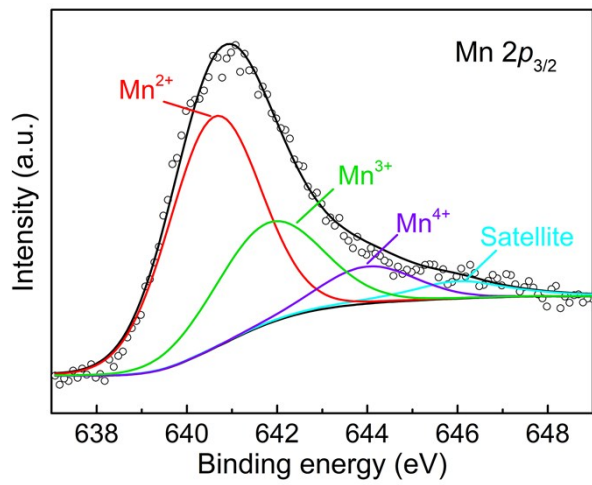


**Fig. S2** The deconvolution of Mn 2p<sub>3/2</sub> XPS spectrum for CaMnMnTaO<sub>6</sub>.

## Supplementary Tables

**Table S1** EDS analysis Ca/Mn/Ta ratios of  $\text{Ca}_{2-x}\text{Mn}_x\text{TaO}_6$  with  $x = 0.4\text{-}1.0$

	$x = 0.4$	$x = 0.6$	$x = 0.8$	$x = 1.0$
Expected ratio	1.6 : 1.4 : 1	1.4 : 1.6 : 1	1.2 : 1.8 : 1	1 : 2 : 1
Observed ratio	1.53 (7) : 1.37 (6) : 1.00 (5)	1.27 (6) : 1.32 (6) : 1.00 (5)	1.19 (5) : 1.87 (9) : 1.00 (5)	0.98 (4) : 1.97 (9) : 1.00 (5)

**Table S2** Structure refinements results of fractional atomic coordinates, occupancies and isotropic displacement parameters ( $\text{\AA}^2$ ) of  $\text{Ca}_{2-x}\text{Mn}_x\text{MnTaO}_6$  with  $x = 0, 0.2, 0.4, 0.6, 0.8$  and  $1.0$

	$x = 0$	$x = 0.2$	$x = 0.4$	$x = 0.6$		$x = 0.8$	$x = 1.0$
				$x = 0.51$	$x = 0.32$		
$a/\text{\AA}$	5.5707 (2)	5.5731 (1)	5.5414 (1)	5.4816 (5)	5.5512 (2)	5.450 (1)	5.4160 (2)
$b/\text{\AA}$	5.4620 (2)	5.4558 (1)	5.4203 (1)	5.4838 (5)	5.4197 (3)	5.4519 (9)	5.4330 (3)
$c/\text{\AA}$	7.7268 (2)	7.7371 (2)	7.7231 (2)	7.7030 (2)	7.7478 (5)	7.7353 (3)	7.7241 (3)
$V/\text{\AA}^3$	235.10 (1)	235.25 (1)	231.966 (8)	231.55 (3)	233.10 (2)	229.85 (6)	227.28 (2)
Ca1/Mn2 4c ( $x, y, 1/4$ )							
$x$	-0.0166 (8)	-0.0262 (8)	-0.0409 (5)	-0.0327 (8)	-0.0377 (13)	0.0325 (10)	0.0315 (10)
$y$	0.0316 (8)	0.0227 (12)	0.0247 (7)	-0.0248 (13)	0.0489 (12)	-0.0379 (8)	-0.0357 (8)
Occ.	1	0.9/0.1	0.8/0.2	0.75/0.25	0.84/0.16	0.6/0.4	0.5/0.5
$B_{\text{iso}}$	2.00 (15)	2.00 (16)	2.0 (2)	2.0 (2)	2.0 (9)	2.0 (2)	2.0 (3)
Mn1/Ta1 4a (1/2, 0, 0)							
$B_{\text{iso}}$	2.44 (14)	2.21 (15)	2.1 (2)	2.5 (2)	2.1 (8)	2.3 (2)	2.7 (3)
O1 4c ( $x, y, 1/4$ )							
$x$	0.0525 (18)	0.050 (2)	0.001 (3)	0.051 (4)	0.024 (6)	-0.044 (6)	-0.034 (5)
$y$	0.481 (3)	0.439 (3)	0.4048 (16)	0.470 (6)	0.469 (4)	0.505 (3)	0.493 (3)
$B_{\text{iso}}$	4.0 (4)	4.0 (5)	4.0 (4)	4.0 (6)	4.0 (11)	3.5 (7)	3.6 (6)
O2 8d ( $x, y, z$ )							
$x$	0.7965 (15)	0.7971 (17)	0.7966 (11)	0.683 (4)	0.794 (3)	0.832 (6)	0.810 (3)
$y$	0.212 (2)	0.210 (2)	0.2120 (14)	0.302 (5)	0.198 (3)	0.180 (7)	0.175 (4)
$z$	0.0496 (8)	0.0385 (13)	-0.0397 (9)	-0.0505 (13)	-0.015 (4)	0.0177 (19)	0.0305 (18)
$B_{\text{iso}}$	1.9 (4)	2.6 (4)	1.9 (3)	3.0 (4)	1.5 (11)	2.1 (4)	4.0 (5)
$R_{\text{wp}} (\%)$	7.93	8.96	5.77	5.42		6.69	8.09
$R_p (\%)$	5.77	6.53	4.25	4.06		4.84	5.78
$\chi^2$	2.35	2.72	2.25	2.12		2.54	3.29

$R_B$ (%)	4.13	4.81	2.72	2.87	2.33	2.64	2.67
-----------	------	------	------	------	------	------	------

---

**Table S3** Selected bond lengths ( $\text{\AA}$ ), BVS and  $(\text{Mn1/Ta1})\text{O}_6$  octahedral distortion parameters of  $\text{Ca}_{2-x}\text{Mn}_x\text{MnTaO}_6$  with  $x = 0, 0.2, 0.4, 0.6, 0.8$  and  $1.0$

	$x = 0$	$x = 0.2$	$x = 0.4$	$x = 0.51^a$	$x = 0.8$	$x = 1.0$
(Ca1/Mn2)-O1	2.485 (17)	2.311 (17)	2.073 (10)	2.75 (3)	2.989 (17)	2.894 (17)
(Ca1/Mn2)-O1	2.600 (11)	2.693 (12)	2.631 (16)	2.64 (2)	2.80 (3)	2.73 (3)
(Ca1/Mn2)-O2 ( $\times 2$ )	2.110 (9)	2.166 (11)	2.473 (7)	2.29 (2)	2.33 (2)	2.372 (17)
(Ca1/Mn2)-O2 ( $\times 2$ )	2.807 (10)	2.805 (11)	2.617 (7)	2.634 (15)	2.42 (3)	2.450 (15)
(Ca1/Mn2)-O2 ( $\times 2$ )	2.938 (8)	2.868 (11)	2.859 (7)	2.89 (2)	3.09 (3)	2.961 (18)
$\langle(\text{Ca1/Mn2})\text{-O1}\rangle$	2.543 (14)	2.502 (15)	2.352 (13)	2.695 (3)	2.895 (10)	2.812 (10)
$\langle(\text{Ca1/Mn2})\text{-O2}\rangle$	2.618 (9)	2.613 (11)	2.650 (7)	2.605 (6)	2.613 (3)	2.594 (17)
$\langle(\text{Ca1/Mn2})\text{-O}\rangle$	2.599 (10)	2.585 (12)	2.575 (9)	2.627 (5)	2.684 (5)	2.649 (15)
BVS(Ca1)	2.14	2.09	1.95	1.61	1.60	1.56
BVS(Mn2)	-	1.29	1.21	1.00	0.99	0.96
BVS(Ca1/Mn2)	2.14	2.01	1.80	1.43	1.36	1.26
(Mn1/Ta1)-O1 ( $\times 2$ )	1.9565 (17)	1.982 (3)	1.999 (2)	1.953 (4)	1.949 (4)	1.940 (3)
(Mn1/Ta1)-O2 ( $\times 2$ )	1.977 (10)	1.967 (10)	1.950 (7)	1.98 (3)	1.98 (4)	1.944 (18)
(Mn1/Ta1)-O2 ( $\times 2$ )	2.053 (9)	2.035 (10)	2.029 (7)	2.09 (2)	2.06 (3)	2.06 (2)
$\langle(\text{Mn1/Ta1})\text{-O1}\rangle$	1.9565 (17)	1.982 (3)	1.999 (2)	1.953 (4)	1.949 (4)	1.940 (3)
$\langle(\text{Mn1/Ta1})\text{-O2}\rangle$	2.015 (10)	2.001 (10)	1.990 (7)	2.035 (3)	2.020 (4)	2.002 (10)
$\langle(\text{Mn1/Ta1})\text{-O}\rangle$	1.996 (12)	1.995 (8)	1.993 (5)	2.008 (3)	1.996 (4)	1.981 (8)
BVS(Mn1)	3.19	3.19	3.21	3.11	3.19	3.33
$\Delta[(\text{Mn1/Ta1})\text{O}_6] \times 10^{-4}$	4.33	2.14	2.67	8.71	5.49	7.89

<sup>a</sup>The data for  $x = 0.51$  phase is shown only in the  $x = 0.6$  case.

**Table S4** Binding energy values and percentage peak areas of the Mn<sup>2+</sup>, Mn<sup>3+</sup> and Mn<sup>4+</sup> calculated from the Mn 2p XPS signals.

	B. E. (eV)	Percentage peak areas (%)	
		Expected value	Observed value
Mn <sup>2+</sup>	640.6	50	60
Mn <sup>3+</sup>	641.8	50	30
Mn <sup>4+</sup>	644.0	0	10

**Table S5** Magnetic parameters of the Curie-Weiss Fits of  $\text{Ca}_{2-x}\text{Mn}_x\text{MnTaO}_6$  ( $x = 0\text{-}1.0$ ) measured in 0.1 T magnetic field.

Compound	$\theta$ (K)	$T_C/T_N$ (K)	$\mu_{\text{eff}}$ ( $\mu_{\text{B}}$ /f.u.)	$\mu_{\text{cal}}$ ( $\mu_{\text{B}}$ /f.u.)
$x = 0$	39.4	19.6	5.33	4.90
$x = 0.2$	23.4	44.0	5.37	5.57
$x = 0.4$	-64.6	11.6	7.69	6.14
$x = 0.6$	-108	16.6	7.59	6.71
$x = 0.8$	-149	22.5	7.94	7.21
$x = 1.0$	-260	23.3	9.55	7.68